



Published in final edited form as:

Hypertension. 2021 February ; 77(2): 507–518. doi:10.1161/HYPERTENSIONAHA.120.16218.

Renovascular disease induces senescence in renal scattered tubular-like cells and impairs their reparative potency

Xiao-Jun Chen^{1,3}, Seo Rin Kim^{1,4}, Kai Jiang¹, Christopher M. Ferguson¹, Hui Tang¹, XiangYang Zhu¹, Amir Lerman², Alfonso Eirin¹, Lilach O. Lerman¹

¹Division of Nephrology and Hypertension, Mayo Clinic, Rochester, MN, USA

²Department of Cardiovascular Diseases, Mayo Clinic, Rochester, MN, USA

³Department of Nephrology, The Second Xiangya Hospital of Central-South University, Changsha, Hunan, China

⁴Division of Nephrology, Pusan National University Yangsan Hospital, Yangsan, Korea

Abstract

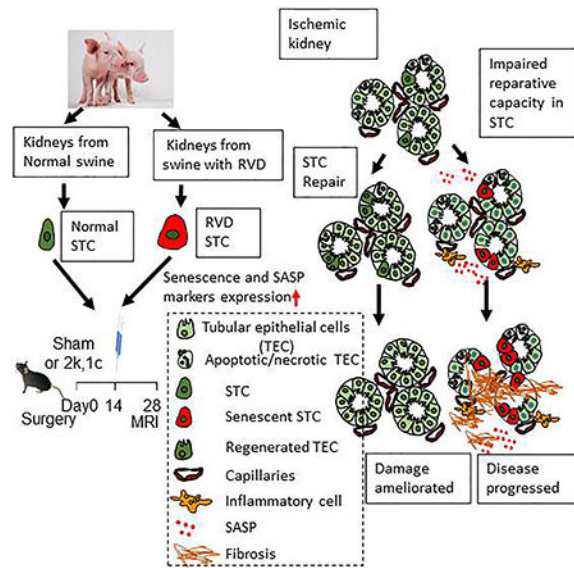
Scattered tubular-like cells (STC), dedifferentiated renal tubular epithelial cells, contribute to renal self-healing, but severe injury might blunt their effectiveness. We hypothesized that ischemic renovascular disease (RVD) induces senescence in STC and impairs their reparative potency. CD24⁺/CD133⁺STC were isolated from swine kidneys after 16 wks of RVD or healthy controls. To test their reparative capabilities in injured kidneys, control or RVD-STC (5×10^5) were pre-labeled and injected into the aorta of 2-kidneys, 1-clip (2k,1c) mice 2 weeks after surgery. Murine renal function and oxygenation were studied in-vivo 2 weeks after injection using micro-magnetic resonance imaging, and fibrosis, tubulointerstitial injury, capillary density, and expression of pro-fibrotic and inflammatory genes ex-vivo. STC isolated from swine RVD kidneys showed increased gene expression of senescence and senescence-associated secretory phenotype markers, and positive SA- β -gal staining. Delivery of normal pig STCs in 2k,1c mice improved murine renal perfusion, blood flow, and glomerular filtration rate, and down-regulated pro-fibrotic and inflammatory gene expression. These renoprotective effects were blunted using STC harvested from RVD kidneys, which also failed to attenuate hypoxia, fibrosis, tubular injury, and capillary loss in injured mouse 2k,1c kidneys. Hence, RVD may induce senescence in endogenous STC and impair their reparative capacity. These observations implicate cellular senescence in the pathophysiology of ischemic kidney disease, and support senolytic therapy to permit self-healing of senescent kidneys.

Graphical Abstract

Correspondence: Lilach O. Lerman, MD, PhD, Division of Nephrology and Hypertension, Mayo Clinic, 200 First Street SW, Rochester, MN 55905. Fax:(507)-266-9316 Phone:(507)-266-9376 lerman.lilach@mayo.edu.

Disclosures

Dr. Lerman is an advisor to AstraZeneca. The authors declare no conflict.



Keywords

Renovascular disease; Renal artery stenosis; Senescence; Scattered tubular-like cells

Introduction

The numbers of senescent cells increase in many forms of renal disease, including acute kidney injury, diabetic nephropathy, and chronic kidney disease¹. During development of senescence, cells undergo a permanent cell-cycle arrest, and adopt a senescence-associated secretory phenotype (SASP), secreting paracrine and autocrine SASP components, including interleukin-6 (IL-6), monocyte attractants, and plasminogen activator inhibitor-1 (PAI-1), that may in turn promote inflammation and fibrosis². Indeed, depletion of senescent cells in experimental kidney disease improves epithelial and microvascular repair and reduced fibrosis³, implying that senescent cells accumulating within the kidney may drive disease progression.

Compared to other cell types, like podocytes, endothelial, and interstitial cells, tubular epithelial cells (TEC) are more susceptible to senescence, as suggested by human kidney biopsy and experimental data^{4, 5}. When stimulated, adult differentiated TEC can transform their phenotype to become reparative CD24⁺/CD133 scattered tubular-like cells (STC) capable of contributing to self-healing of neighboring cells, and ultimately renal recovery⁶. Exogenous delivery of STC or their extracellular vesicles can ameliorate renal function in animal models of renal damage^{7, 8}. Whether renal disease can also transform STC into a senescent phenotype and thereby contribute to maladaptive repair remains unclear.

Renovascular disease (RVD) involves renal artery stenosis leading to intrarenal microvascular and parenchymal damage, resulting in progressive loss of renal function, and possibly cardiovascular events⁹. Furthermore, coexisting metabolic derangements such as metabolic syndrome, which may approach prevalence of 50% in patients with RVD,

amplifies renal damage, favors development of atherosclerosis and thrombosis, and impedes renal recovery¹⁰. We have shown that disease models like murine obesity and swine atherosclerotic RVD trigger renal cellular senescence^{11, 12}, with increased levels of senescence markers like senescence-associated (SA) β -Galactosidase (SA- β -Gal) activity, p16^{Ink4a}, p19^{Arf}, and p21^{CIP1} gene expression, SA heterochromatin foci, and γ H2AX expression. Furthermore, swine RVD induces structural and functional damage in STC mitochondria and impairs their capacity to sustain viability of injured TEC *in-vitro*¹³.

However, the effects of RVD on STC cell-cycle, or on their ability to repair injured kidneys *in-vivo*, remains uncertain. Therefore, we hypothesized that RVD elicits cellular senescence in STC and blunts their reparative potency.

Materials and Methods

The authors declare that all supporting data are available within the article and its online supplementary files. All animal procedures were approved by the Institutional Animal Care and Use Committee.

Experimental Design

To test our hypothesis, we firstly harvested STC from RVD and sham pigs, and characterized their senescence *in-vitro*. We have recently observed that radiation-induced senescent STC cause peritubular endothelial cells loss in healthy mouse kidney¹⁴, probably because senescence renders STC injurious for tubular and neighboring endothelial cells. To verify the impact of RVD-induced senescent STC on endothelial cells *in-vitro*, we co-cultured renal artery endothelial cells (RAEC) and STC in trans-wells and evaluated RAEC protein expression, implicating RVD-induced senescence in cellular injury. To further investigate whether RVD impairs the reparative potency of STC *in-vivo*, we delivered STC in a mouse 2-kidneys,1-clip (2k,1c) model with ischemic kidney injury, and compared the effects of healthy and RVD-STC on renal function and structure.

STC Isolation and cell culture

Kidneys were harvested from six healthy female (6 months-old) and six female age-matched RVD pigs. RVD pigs were firstly fed a high-cholesterol/high-carbohydrate diet (to generate metabolic derangements)¹⁵ for 6 weeks, after which a local irritant coil was placed in their renal artery (to introduce RVD)¹⁶ for 10 additional weeks.

To harvest STC, isolated fresh kidney tissues (4-5g, mainly cortex) were digested as described^{13,17}. CD24⁺/CD133⁺ STC were isolated using CD24 (130-095-951, Miltenyi-Biotec) following a CD133 (130-100-857, Miltenyi-Biotec) MicroBead kits.

Flow cytometry (FlowSight Imaging Flow Cytometer, Amnis, Seattle, WA) was used to identify cells undergoing senescence¹⁸. Cells were stained with SA- β -Gal Staining Kit (#9860, Cell Signaling, Boston, MA)¹¹, run and gated for single cells. Then mean bright-field (BF) pixel intensity was calculated for each event. SA- β -gal-positive (dark with low BF intensity) and SA- β -gal-negative (light-colored with high BF intensity) populations were clearly separated and expressed as percentage of total single cells¹⁴.

Furthermore, STC expressions of senescence-related and SASP genes were studied in total RNA. Quantitative real-time PCR was performed using TaqMan assays (Thermo-Fisher, Waltham, MA): *CDKN2A*(APYMMFE), *CDKN1A*(AJGJQY6), *interleukin (IL)1A*(Ss03391335), *IL6*(Ss03384604), *Bcl-2*(Ss03375167), *C-C motif chemokine-ligand (CCL)-2*(Ss03394377), and *SERPINE1*(Ss03392656), with *TATA-box binding protein (TBP, APCE6HF)* as internal control. Fold-changes of each target gene in the experimental relative to normal STC were calculated using the 2^{-CT} method. Levels of IL-6 (P6000B, R&D systems) and tumor necrosis-factor-alpha (TNF- α , KSC3011, Invitrogen) were measured in conditioned medium by enzyme-linked immunosorbent assay (ELISA) and corrected by the number of cells.

Renal endothelial cells

To isolate primary RAEC¹⁹, a healthy pig renal artery was separated and injected with 2mg/mL collagenase and immediately ligated at both ends. After a 1-hour digestion, the intra-arterial solution was mixed with EGMTM Endothelial Cell Growth Medium (Lonza) and passed through a 100 μ m cell strainer. After centrifugation (1000rpm, 10 minutes), the cell pellet was cultured with EGMTM, which was replaced every 2 days to remove non-adherent cells. After about two weeks, adherent cells were harvested with 0.25% trypsin (Gibco BRL, USA) and cultured. Endothelial phenotype was confirmed by expression of CD31 and Von Willebrand factor¹⁹.

To determine the effects of escalating cellular senescence, RAEC were co-cultured separately with harvested STC found to have a range of 10-30% SA- β -gal-positivity. In a trans-well setup, RAEC (bottom) were separated from STC (top, the same number in each well) with 0%, 10%, or 30% SA- β -gal-positivity. After 48 hours, RAEC protein expression of endothelial nitric oxide synthase (eNOS, 1:50, Abcam) and caspase-8 (1:200, Santa-Cruz) was determined by western blot.

Additional RAEC were cultured in chamber slides with supernatant from STC with 0%, 10%, or 30% SA- β -gal-positivity. After 48 hours, immunoreactivity of eNOS (1:50 Abcam) was measured by immunofluorescent staining and counting eNOS⁺ cells.

In vivo mouse study: Transplantation of STC

C57BL/6J mice (Jackson Lab, Bar Harbor, ME, 11 weeks old) were randomly assigned to Sham (n=6), 2k,1c+Vehicle (n=6), 2k,1c+normal-STC (2k,1c+NSTC, n=8), or 2k,1c+RVD-STC (2k,1c+RSTC, n=8) groups. Animals were anesthetized with 1.75% isoflurane and unilateral 2k,1c induced by placing a tube cuff around the right renal artery, as described⁸. Sham surgeries were performed in controls. This approach leads to ischemic kidney injury, and a fall in renal volume, blood flow, and function. BP was measured at baseline, 2, and 4 weeks after surgery by tail-cuff (Kent Scientific, Torrington, CT). After 2 weeks, through a carotid cannula, 200 μ L PBS or CTFR pre-labeled (far-red, Invitrogen, Waltham, MA) NSTC or RSTC (5X10⁵, 30% SA- β -gal+) slowly injected into the aorta. Two weeks later renal function and oxygenation were assessed using a 16.4-T vertical magnetic resonance imaging (MRI) unit (Bruker Biospin, Billerica, MA), and subsequently mice euthanized with CO₂. Kidneys and blood samples were collected for ex-vivo studies.

Cell tracking.—Frozen kidney tissue embedded in OCT was sectioned at 5 μ m thickness. Potential rejection of the swine STC was evaluated by immunofluorescence staining with CD3 (Abcam)¹⁷. Because they engraft in proximal tubules⁸, STC localization was evaluated by immunofluorescence staining with the proximal tubular marker phaseolus vulgaris erythroagglutinin (PHA-E). To determine whether injected STC proliferate in-vivo, renal sections were stained with Ki67 and PCNA (Abcam). To quantify STC retention rate, cells from fresh stenotic kidney (STK), contralateral kidney (CLK), heart, lung, spleen and liver were prepared²⁰ and analyzed by FACS¹⁷ to count CTFR pre-labeled and DAPI+ cells. The percentage of CTFR+/DAPI+ cells in each organ relative to the total number of DAPI+ cells detected in the six organs was then calculated.

Systemic measurements.—Telemetry transducers interfere with MRI. Therefore, using a XBP1000 system (Kent Scientific, Torrington, CT), systolic blood pressure (SBP) was measured by tail-cuff at baseline, 2, and 4 weeks. Plasma creatinine level and renin content were evaluated using the DetectX® Serum Creatinine kit (Arbor assays, Ann Arbor, MI) and the Angiotensin-I RIA kit (ALPCO, Salem, NH), respectively.

In-vivo renal function.—Two weeks after STC or vehicle injection, kidney volume and perfusion were measured by non-contrast-enhanced MRI²¹, and single-kidney glomerular filtration rate (GFR) by dynamic contrast-enhanced MRI, as described²². Single-kidney volume, perfusion, and GFR were assessed²³. Renal blood flow (RBF) was calculated as the product of renal perfusion and volume, and oxygenation using blood oxygen-level-dependent MRI²⁴, where R_2^* ($1/T_2^*$) is an index of blood oxygenation level.

Histologic analysis.—Fibrosis was estimated in 5- μ m Trichrome stained-slides, and quantified semi-automatically as percent area staining (AxioVision, Carl Zeiss Micro-Imaging, Thornwood, NY) in 10–15 random fields from each section. To evaluate microvascular density, kidneys were stained with anti-CD31 antibody (Cell Signaling, 1:100) and a secondary antibody Alexa Fluoro 594 (Santa-Cruz, 1:100)²⁵. TEC injury (dilation, atrophy, cast formation, sloughing, or basement membrane thickening) was assessed in sections stained with Periodic acid–Schiff slides on a 0–4 scale (0:<10%, 1:10–25%, 2:26–50%, 3:51–75% and 4:>75% injury)²⁶. Apoptosis was assessed in renal sections stained with terminal deoxynucleotidyl transferase dUTP nick-end labeling (TUNEL, Promega), and the ratio of TUNEL+ cells relative to total DAPI-stained nuclei calculated. All slides were analyzed in a blinded manner.

Real-time PCR.—Pro-fibrotic and inflammatory genes were studied in RNA isolated from frozen mouse kidney tissue. Quantitative PCR was done using TaqMan probes (Thermo-Fisher Scientific): *Serpine1*(PAI-1, mm00436753), *Ccl2*(monocyte chemotactic protein 1, MCP-1, mm00441242), and *TATA-box binding protein* (*Tbp*, mm01277042) as an internal control.

Statistical analysis

Statistical analysis used the JMP software. Data are expressed as mean \pm SD or median (range). Statistical significance was assessed by one-way analysis of variance followed by

unpaired t-test for normally distributed data or nonparametric (Wilcoxon and Kruskal-Wallis) test for non-normally distributed data. Paired t-test was performed within group comparison. A $p < 0.05$ was considered significant.

Results

RVD induced STC senescence

All RVD pigs developed significant stenosis and hypertension. Renal STC from RVD swine seemed morphologically larger than normal STC and stained positive with SA- β -gal (Fig. 1A). As per flow cytometry with SA- β -gal staining, $28 \pm 12\%$ of RSTC were senescent (Fig. 1A), compared to $0.04 \pm 0.02\%$ of NSTC. Furthermore, RSTC showed increased expression of mRNA characteristic of senescence (*CDKN2A*, $p=0.05$, Fig. 1B), SASP markers (*IL-6*, $p<0.01$, *Ccl2*, and *Serpine1*, both $p=0.02$), and anti-apoptosis (*Bcl-2*, $p=0.02$), whereas *CDKN1A* and *IL1 α* were unchanged (Fig. 1B). IL-6 level was elevated in conditioned-medium from RSTC compared to NSTC ($p=0.02$), whereas TNF- α level was not statistically different (supplementary Fig.S1A).

Impact of STC on RAEC *ex-vivo*

RAEC co-cultured both with 10% and 30% SA- β -gal-positive STC showed decreased expression of eNOS (both $p<0.01$ vs. 0%, Fig. 2A–B). Furthermore, culture with STC supernatant induced a dose-dependent decrease in RAEC eNOS expression that paralleled the extent of STC senescence (per %SA- β -gal-positivity, each $p<0.001$ compared to other doses, Fig. 2C–D).

The expression of caspase-8 increased only when co-cultured with 30% SA- β -gal+ STC ($p=0.3$ for 10% vs. 0%).

STC mainly engraft in the 2k,1c kidney

Two weeks after injection, cells were detected engrafted in the mouse kidneys, especially in TEC, and no co-localization with CD+3 T-cells indicated no obvious signs of immune response (Figure 3A). Engrafted STC co-stained with PCNA and Ki67 indicated their proliferation *in-vivo*. Flow cytometry revealed that NSTC and RSTC engrafted to a similar extent, and showed preferential engraftment in STK compared to CLK and other organs (all $p<0.001$, Figure 3B).

Renoprotective effects were blunted in RSTC-treated mice

The 2k,1c mice showed a similar rise in SBP 2 weeks after surgery (all $p < 0.01$ vs. baseline, Figure 4A). RSTC increased BP at 4-weeks ($p=0.03$ vs. 2 weeks), as well as plasma renin content ($p < 0.02$ vs. other groups, Figure 3B). Elevated creatinine levels in 2k,1c+Vehicle 4 weeks after surgery were unaffected by treatment (all $p < 0.02$ vs. sham, supplementary Fig.S1B).

MRI showed a comparable decreased ratio of STK/CLK volumes among the 2k,1c groups, suggesting a similar degree of stenosis (supplementary Fig.S1C). Compared to sham, STK perfusion, RBF, and GFR was decreased in all the groups ($p<0.0001$ vs. Sham), while renal

cortical hypoxia by BOLD-MRI was elevated ($p=0.009$, Fig. 4C–F). However, compared to 2k,1c, NSTC significantly improved RBF and GFR ($p=0.05$ and 0.04 vs. 2k,1c+Vehicle, respectively), and tended to increase renal perfusion and ameliorate cortical hypoxia ($p=0.07$ and 0.09 vs. 2k,1c, respectively). Contrarily, RSTC did not attenuate renal cortical hypoxia ($p>0.1$ vs. 2k,1c+Vehicle), and renal perfusion, RBF, and GFR were all lower than in 2k,1c+NSTC ($p<0.05$).

RSTC do not ameliorate STK structural damage

Trichrome staining demonstrated marked fibrosis in untreated STKs, which was significantly alleviated by NSTC ($p=0.04$ vs 2k,1c+Vehicle, Fig 5A–B), but not by RSTC ($p=0.3$ vs 2k,1c+Vehicle), and neither was tubular injury by PAS staining (Fig 5A,C). Fewer CD31+ capillary endothelial cells per tubule in 2k,1c compared with Sham implied STK capillary loss ($p<0.001$, Fig5A, D), which was improved in 2k,1c+NSTC ($p=0.02$ vs 2k,1c+Vehicle), but remained decreased in 2k,1c+RSTC ($p=0.2$ vs 2k,1c+Vehicle). STK PAI-1 (*serpine1*) and MCP-1 (*ccl2*) gene expression was up-regulated in 2k,1c+Vehicle ($p=0.02$ and 0.009 vs Sham, respectively, Fig 5D) and significant down-regulated by NSTC ($p=0.02$ and 0.004 vs 2k,1c+Vehicle, respectively), but not by RSTC ($p=0.4$ and 0.2 vs 2k,1c+Vehicle, respectively). TUNEL staining showed increased apoptosis in untreated STKs, which was significantly decreased by NSTC ($p=0.05$ vs 2k,1c+Vehicle, Fig 5A–B), but not by RSTC ($p=0.3$ vs 2k,1c+Vehicle) (supplementary Fig.S1D).

Discussion

This study demonstrates that RVD, a swine model emulating human disease, induces senescence in endogenous STC, and impairs their reparative capacity both *in-vivo* and *in-vitro*. Consequently, while exogenous delivery of STC harvested from healthy swine kidneys improves structure and function in ischemic mouse kidneys, these salutary effects were abolished in 2k,1c mice treated with STC from RVD pigs. Similarly, proportionally to their extent of senescence, RSTC altered protein expression in renal endothelial cells *in-vitro*. These observations implicate STC senescence in maladaptive renal self-repair that may contribute to kidney disease progression.

Cellular senescence involves irreversible arrest of cell proliferation and development of SASP, observed in many renal diseases³. TEC are particularly susceptible to senescence, and may mediate maladaptive repair during progression of chronic injury²⁷. The paracrine effects of senescent cells contribute to fibrosis, inflammation, and stem/progenitor cell dysfunction²⁸. Progenitor cells like STC also proliferate and differentiate to support injured TEC during renal repair^{29, 30}. We have previously shown that metabolic burden and renal ischemia, the chief kidney insults in RVD, led to decreased STC capacity for proliferation¹³ and down-regulation of genes encoding for cell-cycle and cytoskeleton³¹. The present study extends our previous studies to show that RVD induces senescence in STC, evidenced by increased senescence (SA- β -Gal, p16^{Ink4a}) and SASP (IL-6, MCP-1, PAI-1) markers, and upregulates gene expression of Bcl-2, indicating resistance to apoptosis characterizing senescent cells³². Development of STC senescence may be related to mitochondrial dysfunction and increased production of reactive oxygen species³³, which are observed in

RSTC¹³. While CDKN1A (p21^{CIP1}) gene expression was not different between normal and RSTC, it might be an early trigger of senescence³² and does not necessarily persist³⁴, whereas p16^{Ink4a} is activated later to maintain the senescent state³².

The current study shows in RSTC upregulated expression of pro-inflammatory factors, including *il-6*, *ccl2*, and *serpine*. We have previously found elevated mitochondrial biogenesis and expression of mitomiRs targeting mtDNA-genes in RSTC³⁵, as well as mRNAs encoding for proteins involved in cell adhesion and matrix remodeling³¹. Hence, STC may exhibit altered modulation of mitochondria-related gene expression, cell adhesion, and fibrogenic activity.

Cellular senescence can abrogate the therapeutic potential of stem/progenitor cells³⁶ by impairing their migratory, differentiation, and immunomodulation ability³⁷. Therefore, we hypothesized that STC from RVD swine would exhibit diminished protective effects in murine 2k,1c. More STC engrafted in the STK than CLK, likely secondary to upregulated homing factors and adhesion molecules in injured kidneys³⁸. Normal STC ameliorated STK fibrosis and tubular injury, and in turn STK-RBF and GFR. The mechanism probably involves not only STC engraftment, but mainly paracrine mechanisms, including release of soluble factors like IL-15, a kidney-specific factor involved in renal differentiation⁷, and STC-derived extracellular vehicles that shuttle their cargo⁸. Furthermore, STC improve the renal microvasculature by releasing growth factors⁷ and attenuating oxidative stress and inflammation. Thus, STC-induced microvascular proliferation, as indicated in increased number of peritubular capillaries, likely augmented renal perfusion and attenuated hypoxia in 2k,1c+NSTC. In particular, robust pro-angiogenic effects of STC may result from repair of TEC, evidenced by decreased injury score, which supports maintenance of tubulo-vascular cross-talk³⁹ and sustains the peri-tubular capillary and microvascular networks.

Contrarily, although only 30% of delivered RSTC were senescent, they failed to achieve a therapeutic effect on murine STK structure and function. This deficiency might have resulted partly from their inability to downregulate STK gene expression of PAI-1 and MCP-1. PAI-1 is implicated in renal fibrosis⁴⁰, while pro-inflammatory MCP-1 contributes to STK injury and dysfunction⁴¹. Importantly, we have recently shown that exogenous senescent STC delivery can directly injure healthy mouse kidneys¹⁴, an impact which might have offset the reparative effect of non-senescent STC. Furthermore, this might have been masked in 2k,1c+RSTC, due to the background of substantial renal injury observed in 2k,1c alone.

Interestingly, RSTC in fact elevated SBP at 4-weeks compared with 2-week, whereas NSTC or vehicle did not. Similarly, renin level in RSTC-treated mice was higher than all other groups, possibly due to direct activation of the renin-angiotensin system by the intra-renal inflammatory milieu. Additionally, when co-cultured *in-vitro* with RSTC, RAEC showed lower expression of eNOS and higher expression of an apoptosis mediator (caspase-8). In endothelial cells eNOS produces nitric oxide that maintains their integrity and plays an antihypertensive role⁴². Apoptosis of RAEC can also lead to capillary rarefaction implicated in the pathogenesis of hypertension⁴³. Thus, RSTC might induce endothelial cell dysfunction and loss, which further exacerbates hypertension. Notably, the extent of SA-β-

gal+ in STC or their supernatant influenced their impact on caspase-8 and eNOS expression in RAEC. This dose-response relationship is consistent with the implicit role of RVD-induced senescence in disease progression.

We acknowledge some limitations in our study. Firstly, the RVD model is composed of young pigs, and shorter disease duration than in humans, yet recapitulates the ischemic and metabolic components of RVD that effectively modified the STC. Secondly, to observe impact of RVD, we used xenogeneic renal STC, which might be associated with rejection, although rejection was not observed in CD3 staining. Additionally, the relative contribution of senescence to maladaptive renal repair remains to be elucidated, since the overall population of STC in RVD kidney is relatively small (5.9%)¹³, as is the portion of senescent STC. Nevertheless, 1/10,000 transplanted senescent cells are sufficient to cause deleterious effects⁴⁴. Moreover, senescent cells can drive surrounding cells into inflammation or senescence by paracrine release of SASP²⁸, while the intrinsic anti-apoptotic attributes of senescent cells may help extend their own survival⁴⁵ and thereby perpetuate their impact. Lastly, in 2k,1c+Vehicle renin level was unaltered, since it can return to normal levels at chronic phases of renal ischemia⁴⁶. Despite normalized PRA in 2K1C mice, elevated intrarenal renin activity at 4-6 weeks⁴⁷⁻⁵⁰ may account for maintenance of hypertension⁵¹.

Summary

STC isolated from swine RVD kidneys showed increased gene expression of senescence and senescence-associated secretory phenotype markers, and positive SA- β -gal staining. Delivery of normal pig STCs in 2k,1c mice improved murine renal perfusion, blood flow, and glomerular filtration rate, and down-regulated pro-fibrotic and inflammatory gene expression. These renoprotective effects were blunted using STC harvested from RVD kidneys, which also failed to attenuate hypoxia, fibrosis, tubular injury, and loss of capillaries in injured mouse 2k,1c kidneys.

Perspectives

In conclusion, our study shows that experimental RVD leads to senescence in STC, which is characterized by increased senescence and SASP markers. STC from RVD swine also show negative impact on endothelial cells *in-vitro* and impaired capacity to repair ischemic mouse kidneys *in-vivo*. These observations implicate senescence in inadequate renal self-healing, and support novel intervention strategies targeting renal senescence in kidney disease.

Supplementary Material

Refer to Web version on PubMed Central for supplementary material.

Acknowledgements

Sources of Funding

This study was partly supported by NIH grant numbers DK120292, DK104273, DK122734, DK102325, DK106427, and DK122137.

References

1. Sturmlechner I, Durik M, Sieben CJ, Baker DJ, van Deursen JM. Cellular senescence in renal ageing and disease. *Nat Rev Nephrol.* 2017; 13:77–89. doi: 10.1038/nrneph.2016.183. [PubMed: 28029153]
2. Zhu Y, Armstrong JL, Tchkonina T, Kirkland JL. Cellular senescence and the senescent secretory phenotype in age-related chronic diseases. *Curr Opin Clin Nutr Metab Care.* 2014; 17:324–328. doi: 10.1097/MCO.000000000000065. [PubMed: 24848532]
3. Docherty MH, O'Sullivan ED, Bonventre JV, Ferenbach DA. Cellular senescence in the kidney. *J Am Soc Nephrol.* 2019; 30:726–736. doi: 10.1681/ASN.2018121251. [PubMed: 31000567]
4. Liu J, Yang JR, He YN, Cai GY, Zhang JG, Lin LR, Zhan J, Zhang JH, Xiao HS. Accelerated senescence of renal tubular epithelial cells is associated with disease progression of patients with immunoglobulin a (iga) nephropathy. *Transl Res.* 2012; 159:454–463. doi: 10.1016/j.trsl.2011.11.008. [PubMed: 22633096]
5. Sis B, Tasanarong A, Khoshjou F, Dadras F, Solez K, Halloran PF. Accelerated expression of senescence associated cell cycle inhibitor p16ink4a in kidneys with glomerular disease. *Kidney Int.* 2007; 71:218–226. doi: 10.1038/sj.ki.5002039. [PubMed: 17183247]
6. Romagnani P, Remuzzi G. Cd133+ renal stem cells always co-express cd24 in adult human kidney tissue. *Stem Cell Res.* 2014; 12:828–829. doi: 10.1016/j.scr.2013.12.011. [PubMed: 24467938]
7. Grange C, Moggio A, Tapparo M, Porta S, Camussi G, Bussolati B. Protective effect and localization by optical imaging of human renal cd133+ progenitor cells in an acute kidney injury model. *Physiol Rep.* 2014; 2:e12009. doi: 10.14814/phy2.12009. [PubMed: 24793983]
8. Zou X, Kwon SH, Jiang K, Ferguson CM, Puranik AS, Zhu X, Lerman LO. Renal scattered tubular-like cells confer protective effects in the stenotic murine kidney mediated by release of extracellular vesicles. *Sci Rep.* 2018; 8:1263. doi: 10.1038/s41598-018-19750-y. [PubMed: 29352176]
9. Lerman L, Textor SC. Pathophysiology of ischemic nephropathy. *Urol Clin North Am.* 2001; 28:793–803. doi: 10.1016/s0094-0143(01)80034-3. [PubMed: 11791495]
10. Davies MG, Saad WE, Bismuth J, Naoum JJ, Peden EK, Lumsden AB. Impact of metabolic syndrome on the outcomes of percutaneous renal angioplasty and stenting. *J Vasc Surg.* 2010; 51:926–932. doi: 10.1016/j.jvs.2009.09.042. [PubMed: 20022208]
11. Kim SR, Jiang K, Ogrodnik M, Chen X, Zhu XY, Lohmeier H, Ahmed L, Tang H, Tchkonina T, Hickson LJ, Kirkland JL, Lerman LO. Increased renal cellular senescence in murine high-fat diet: Effect of the senolytic drug quercetin. *Transl Res.* 2019; 213:112–123. doi: 10.1016/j.trsl.2019.07.005. [PubMed: 31356770]
12. Kim SR, Eirin A, Zhang X, Lerman A, Lerman LO. Mitochondrial protection partly mitigates kidney cellular senescence in swine atherosclerotic renal artery stenosis. *Cell Physiol Biochem.* 2019; 52:617–632. doi: 10.33594/000000044 [PubMed: 30907989]
13. Nargesi AA, Zhu XY, Conley SM, Woollard JR, Saadiq IM, Lerman LO, Eirin A. Renovascular disease induces mitochondrial damage in swine scattered tubular cells. *Am J Physiol Renal Physiol.* 2019; 317:F1142–F1153. doi: 10.1152/ajprenal.00276.2019. [PubMed: 31461348]
14. Kim SR, Jiang K, Ferguson CM, Tang H, Chen XJ, Zhu XY, Hickson LJ, Tchkonina T, Kirkland JL, Lerman LO. Transplanted senescent renal scattered tubular-like cells induce injury in the mouse kidney. *Am J Physiol Renal Physiol.* 2020; 318: F1167–F1176. doi: 10.1152/ajprenal.00535.2019. [PubMed: 32223312]
15. Pawar AS, Zhu XY, Eirin A, Tang H, Jordan KL, Woollard JR, Lerman A, Lerman LO. Adipose tissue remodeling in a novel domestic porcine model of diet-induced obesity. *Obesity (Silver Spring).* 2015; 23:399–407. doi: 10.1002/oby.20971. [PubMed: 25627626]
16. Lerman LO, Schwartz RS, Grande JP, Sheedy PF, Romero JC. Noninvasive evaluation of a novel swine model of renal artery stenosis. *J Am Soc Nephrol.* 1999; 10:1455–1465. [PubMed: 10405201]
17. Zou X, Jiang K, Puranik AS, Jordan KL, Tang H, Zhu X, Lerman LO. Targeting murine mesenchymal stem cells to kidney injury molecule-1 improves their therapeutic efficacy in chronic ischemic kidney injury. *Stem Cells Transl Med.* 2018; 7:394–403. doi: 10.1002/sctm.17-0186. [PubMed: 29446551]

18. Biran A, Zada L, Abou Karam P, Vadai E, Roitman L, Ovadya Y, Porat Z, Krizhanovsky V. Quantitative identification of senescent cells in aging and disease. *Aging Cell*. 2017; 16:661–671. doi: 10.1111/ace.12592. [PubMed: 28455874]
19. Eirin A, Ebrahimi B, Zhang X, Zhu XY, Woollard JR, He Q, Textor SC, Lerman A, Lerman LO. Mitochondrial protection restores renal function in swine atherosclerotic renovascular disease. *Cardiovasc Res*. 2014; 103:461–472. doi: 10.1093/cvr/cvu157. [PubMed: 24947415]
20. Aghajani Nargesi A, Zhu XY, Conley SM, Woollard JR, Saadiq IM, Lerman LO, Eirin A. Renovascular disease induces mitochondrial damage in swine scattered tubular cells. *Am J Physiol Renal Physiol*. 2019; 317: F1142–F1153. doi: 10.1152/ajprenal.00276.2019. [PubMed: 31461348]
21. Jiang K, Ponzo TA, Tang H, Mishra PK, Macura SI, Lerman LO. Multiparametric mri detects longitudinal evolution of folic acid-induced nephropathy in mice. *Am J Physiol Renal Physiol*. 2018; 315:F1252–F1260. doi: 10.1152/ajprenal.00128.2018. [PubMed: 30089037]
22. Jiang K, Tang H, Mishra PK, Macura SI, Lerman LO. Measurement of murine single-kidney glomerular filtration rate using dynamic contrast-enhanced mri. *Magn Reson Med*. 2018; 79:2935–2943. doi: 10.1002/mrm.26955. [PubMed: 29034514]
23. Jiang K, Tang H, Mishra PK, Macura SI, Lerman LO. Measurement of murine kidney functional biomarkers using dce-mri: A multi-slice tricks technique and semi-automated image processing algorithm. *Magn Reson Imaging*. 2019; 63:226–234. doi: 10.1016/j.mri.2019.08.029. [PubMed: 31442558]
24. Jiang K, Ferguson CM, Ebrahimi B, Tang H, Kline TL, Burningham TA, Mishra PK, Grande JP, Macura SI, Lerman LO. Noninvasive assessment of renal fibrosis with magnetization transfer mr imaging: Validation and evaluation in murine renal artery stenosis. *Radiology*. 2016; 283: 77–86. doi: 10.1148/radiol.2016160566. [PubMed: 27697008]
25. Sweetwyne MT, Pippin JW, Eng DG, Hudkins KL, Chiao YA, Campbell MD, Marcinek DJ, Alpers CE, Szeto HH, Rabinovitch PS, Shankland SJ. The mitochondrial-targeted peptide, ss-31, improves glomerular architecture in mice of advanced age. *Kidney Int*. 2017; 91:1126–1145. doi: 10.1016/j.kint.2016.10.036. [PubMed: 28063595]
26. Chen XJ, Zhang X, Jiang K, Krier JD, Zhu X, Lerman A, Lerman LO. Improved renal outcomes after revascularization of the stenotic renal artery in pigs by prior treatment with low-energy extracorporeal shockwave therapy. *J Hypertens*. 2019; 37:2074–2082. doi: 10.1097/HJH.0000000000002158. [PubMed: 31246892]
27. Li Y, Lerman LO. Cellular senescence: A new player in kidney injury. *Hypertension*. 2020; 76:1069–1075. doi: 10.1161/HYPERTENSIONAHA.120.14594. [PubMed: 32862712]
28. Tchkonja T, Kirkland JL. Aging, cell senescence, and chronic disease: Emerging therapeutic strategies. *JAMA*. 2018; 320:1319–1320. doi: 10.1001/jama.2018.12440 [PubMed: 30242336]
29. Smeets B, Boor P, Dijkman H, Sharma SV, Jirak P, Mooren F, Berger K, Bornemann J, Gelman IH, Floege J, van der Vlag J, Wetzels JF, Moeller MJ. Proximal tubular cells contain a phenotypically distinct, scattered cell population involved in tubular regeneration. *J Pathol*. 2013; 229:645–659. doi: 10.1002/path.4125. [PubMed: 23124355]
30. Lindgren D, Bostrom AK, Nilsson K, Hansson J, Sjolund J, Moller C, Jirstrom K, Nilsson E, Landberg G, Axelson H, Johansson ME. Isolation and characterization of progenitor-like cells from human renal proximal tubules. *Am J Pathol*. 2011; 178:828–837. doi: 10.1016/j.ajpath.2010.10.026. [PubMed: 21281815]
31. Aghajani Nargesi A, Zhu XY, Liu Y, Tang H, Jordan KL, Lerman LO, Eirin A. Renal artery stenosis alters gene expression in swine scattered tubular-like cells. *Int J Mol Sci*. 2019; 20:5069. doi: 10.3390/ijms20205069.
32. Herranz N, Gil J. Mechanisms and functions of cellular senescence. *J Clin Invest*. 2018; 128:1238–1246. doi: 10.1172/JCI95148. [PubMed: 29608137]
33. Ziegler DV, Wiley CD, Velarde MC. Mitochondrial effectors of cellular senescence: Beyond the free radical theory of aging. *Aging Cell*. 2015; 14:1–7. doi: 10.1111/ace.12287. [PubMed: 25399755]
34. Sharpless NE, Sherr CJ. Forging a signature of in vivo senescence. *Nat Rev Cancer*. 2015; 15:397–408. doi: 10.1038/nrc3960. [PubMed: 26105537]

35. Farahani RA, Zhu XY, Tang H, Jordan KL, Lerman LO, Eirin A. Renal ischemia alters expression of mitochondria-related genes and impairs mitochondrial structure and function in swine scattered tubular-like cells. *Am J Physiol Renal Physiol*. 2020; 319:F19–F28. doi: 10.1152/ajprenal.00120.2020. [PubMed: 32463728]
36. Turinetto V, Vitale E, Giachino C. Senescence in human mesenchymal stem cells: Functional changes and implications in stem cell-based therapy. *Int J Mol Sci*. 2016; 17:1164. doi:10.3390/ijms17071164..
37. Gnani D, Crippa S, Della Volpe L, Rossella V, Conti A, Lettera E, Ravis S, Ometti M, Frascini G, Bernardo ME, Di Micco R. An early-senescence state in aged mesenchymal stromal cells contributes to hematopoietic stem and progenitor cell clonogenic impairment through the activation of a pro-inflammatory program. *Aging Cell*. 2019; 18:e12933. doi: 10.1111/ace1.12933. [PubMed: 30828977]
38. Chade AR, Zhu XY, Krier JD, Jordan KL, Textor SC, Grande JP, Lerman A, Lerman LO. Endothelial progenitor cells homing and renal repair in experimental renovascular disease. *Stem Cells*. 2010; 28:1039–1047. doi: 10.1002/stem.426. [PubMed: 20506499]
39. Dimke H, Sparks MA, Thomson BR, Frische S, Coffman TM, Quaggin SE. Tubulovascular cross-talk by vascular endothelial growth factor maintains peritubular microvasculature in kidney. *J Am Soc Nephrol*. 2015; 26:1027–1038. doi: 10.1681/ASN.2014010060. [PubMed: 25385849]
40. Ghosh AK, Vaughan DE. Pai-1 in tissue fibrosis. *J Cell Physiol*. 2012; 227:493–507. doi: 10.1002/jcp.22783. [PubMed: 21465481]
41. Zhu XY, Chade AR, Krier JD, Daghini E, Lavi R, Guglielmotti A, Lerman A, Lerman LO. The chemokine monocyte chemoattractant protein-1 contributes to renal dysfunction in swine renovascular hypertension. *J Hypertens*. 2009; 27:2063–2073. doi: 10.1097/HJH.0b013e3283300192. [PubMed: 19730125]
42. Li Q, Youn JY, Cai H. Mechanisms and consequences of endothelial nitric oxide synthase dysfunction in hypertension. *J Hypertens*. 2015; 33:1128–1136. doi: 10.1097/HJH.0000000000000587 [PubMed: 25882860]
43. Afsar B, Afsar RE, Dagele T, Kaya E, Erus S, Ortiz A, Covic A, Kanbay M. Capillary rarefaction from the kidney point of view. *Clin Kidney J*. 2018; 11:295–301. doi: 10.1093/ckj/sfx133. [PubMed: 29988260]
44. Xu M, Pirtskhalava T, Farr JN, Weigand BM, Palmer AK, Weivoda MM, Inman CL, Ogrodnik MB, Hachfeld CM, Fraser DG, Onken JL, Johnson KO, Verzosa GC, Langhi LGP, Weigl M, Giorgadze N, LeBrasseur NK, Miller JD, Jurk D, Singh RJ, Allison DB, Ejima K, Hubbard GB, Ikeno Y, Cubro H, Garovic VD, Hou X, Weroha SJ, Robbins PD, Niedernhofer LJ, Khosla S, Tchkonja T, Kirkland JL. Senolytics improve physical function and increase lifespan in old age. *Nat Med*. 2018; 24:1246–1256. doi: 10.1038/s41591-018-0092-9. [PubMed: 29988130]
45. Xu M, Bradley EW, Weivoda MM, Hwang SM, Pirtskhalava T, Decklever T, Curran GL, Ogrodnik M, Jurk D, Johnson KO, Lowe V, Tchkonja T, Westendorf JJ, Kirkland JL. Transplanted senescent cells induce an osteoarthritis-like condition in mice. *J Gerontol A Biol Sci Med Sci*. 2017; 72:780–785. doi: 10.1093/gerona/glw154. [PubMed: 27516624]
46. Lerman LO, Nath KA, Rodriguez-Porcel M, Krier JD, Schwartz RS, Napoli C, Romero JC. Increased oxidative stress in experimental renovascular hypertension. *Hypertension*. 2001; 37:541–546. doi: 10.1161/01.hyp.37.2.541. [PubMed: 11230332]
47. Warner GM, Cheng J, Knudsen BE, Gray CE, Deibel A, Juskewitch JE, Lerman LO, Textor SC, Nath KA, Grande JP. Genetic deficiency of smad3 protects the kidneys from atrophy and interstitial fibrosis in 2k1c hypertension. *Am J Physiol Renal Physiol*. 2012; 302:F1455–1464. doi: 10.1152/ajprenal.00645.2011. [PubMed: 22378822]
48. Cervenka L, Vaneckova I, Huskova Z, Vanourkova Z, Erbanova M, Thumova M, Skaroupkova P, Opocensky M, Maly J, Chabova VC, Tesar V, Burgelova M, Viklicky O, Teplan V, Zelizko M, Kramer HJ, Navar LG. Pivotal role of angiotensin ii receptor subtype 1a in the development of two-kidney, one-clip hypertension: Study in angiotensin ii receptor subtype 1a knockout mice. *J Hypertens*. 2008; 26:1379–1389. doi: 10.1097/HJH.0b013e3282fe6eaa. [PubMed: 18551014]
49. Dias AT, Cintra AS, Frossard JC, Palomino Z, Casarini DE, Gomes IB, Balarini CM, Gava AL, Campagnaro BP, Pereira TM, Meyrelles SS, Vasquez EC. Inhibition of phosphodiesterase 5

- restores endothelial function in renovascular hypertension. *J Transl Med.* 2014; 12:250. doi: 10.1186/s12967-014-0250-x. [PubMed: 25223948]
50. Hartono SP, Knudsen BE, Zubair AS, Nath KA, Textor SJ, Lerman LO, Grande JP. Redox signaling is an early event in the pathogenesis of renovascular hypertension. *Int J Mol Sci.* 2013; 14:18640–18656. doi: 10.3390/ijms140918640. [PubMed: 24025423]
51. Kim YG, Lee SH, Kim SY, Lee A, Moon JY, Jeong KH, Lee TW, Lim SJ, Sohn IS, Ihm CG. Sequential activation of the intrarenal renin-angiotensin system in the progression of hypertensive nephropathy in goldblatt rats. *Am J Physiol Renal Physiol.* 2016; 311:F195–206. doi: 10.1152/ajprenal.00001.2015. [PubMed: 26823279]

Novelty and Significance

What Is New?

Experimental renovascular disease (RVD) leads to senescence in scattered tubular-like cells (STC), characterized by increased senescence and senescence-associated secretory phenotype markers. STC from RVD swine also injured endothelial cells in-vitro and showed impaired capacity to repair ischemic mouse kidneys in-vivo.

What Is Relevant?

RVD, a leading cause of renovascular hypertension, may transform STC into a senescent phenotype and thereby contribute to maladaptive kidney repair.

Summary

Our study suggests that senescence is involved in inadequate renal self-healing, and supports novel interventional strategies targeting renal senescence in kidney disease.

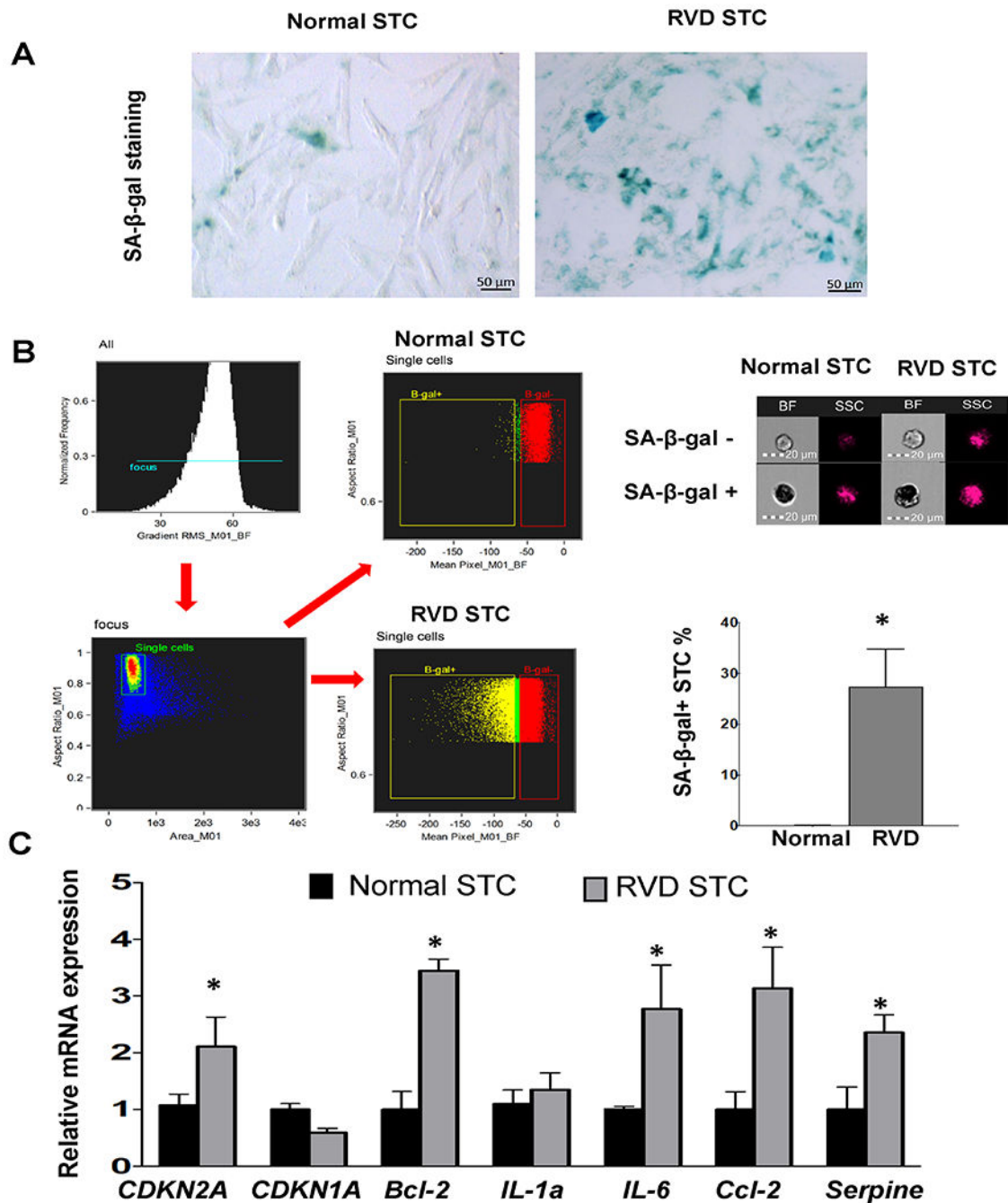


Fig. 1. Characterization of renal scattered tubular-like cells (STC) from Normal and RVD pigs. A, Representative senescence-associated β -galactosidase (SA- β -Gal) staining of STC (Blue). B, Flow cytometry strategy: single-cells were gated first, and then mean bright field (BF) pixel intensity calculated for each event. SA- β -gal-positive (dark cells, low BF intensity) and SA- β -gal-negative (light-colored, high BF) populations were finally gated, expressed as percentage of total single-cells. The percentages of SA- β -gal-positive STC in RVD was

higher than in Normal swine. C, Gene expression of senescence and SASP factors quantified by RT-PCR (relative to *TBP*). Mean±SD; Normal n=5-6, RVD n=5-6; *p<0.05 vs. Normal.

Author Manuscript

Author Manuscript

Author Manuscript

Author Manuscript

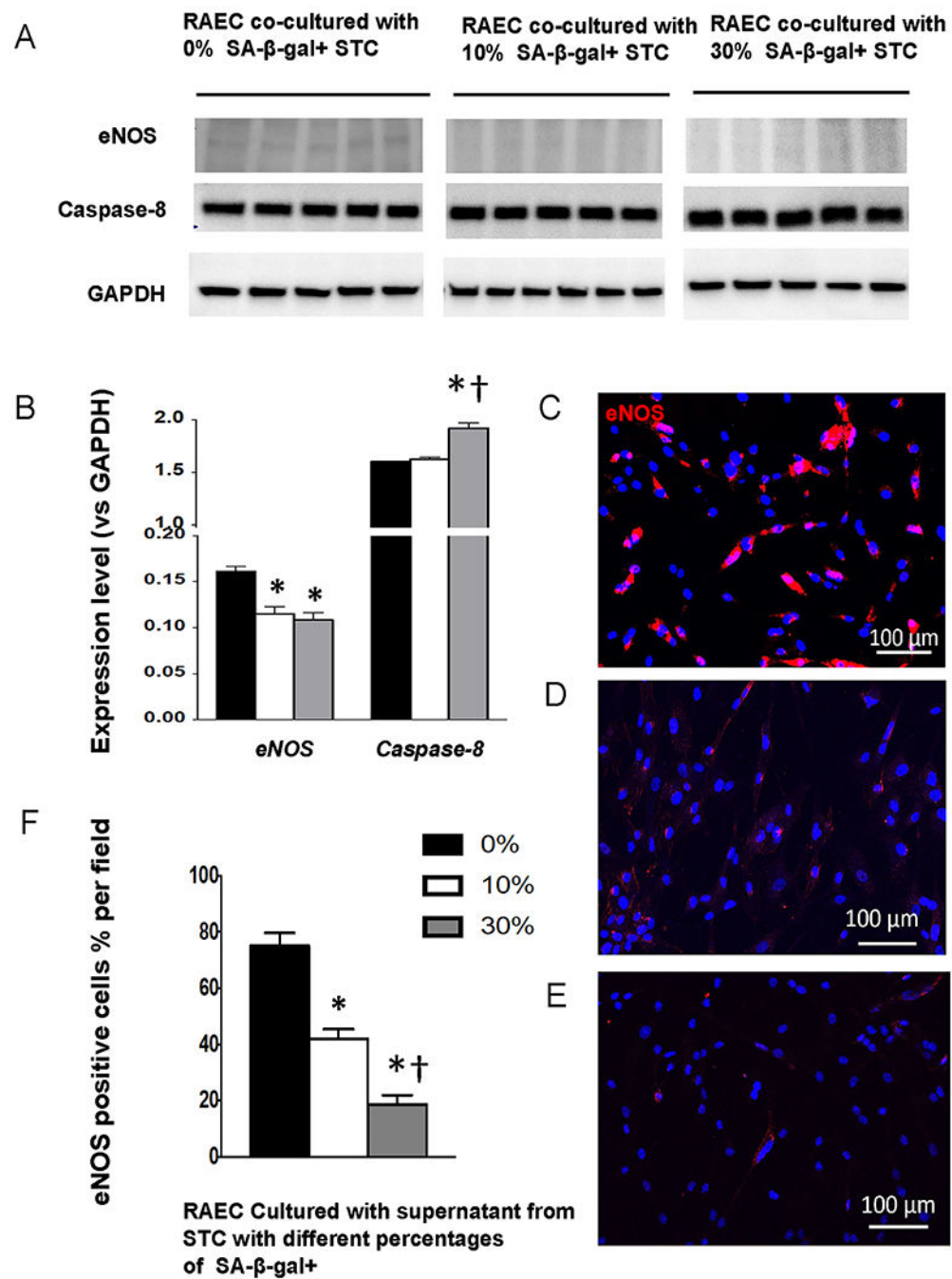


Fig. 2. A-B, Expression of eNOS and caspase-8 in renal artery endothelial cells (RAEC) co-cultured with 0%, 10%, or 30% (n=5 each) SA-β-Gal-positive STC. C-F, Immunoreactivity of eNOS (magenta) in RAEC cultured with STC supernatant falls progressively with increasing fractions of SA-β-gal+. Mean±SD; *p<0.05 vs. 0%, †p<0.05 vs. 10%.

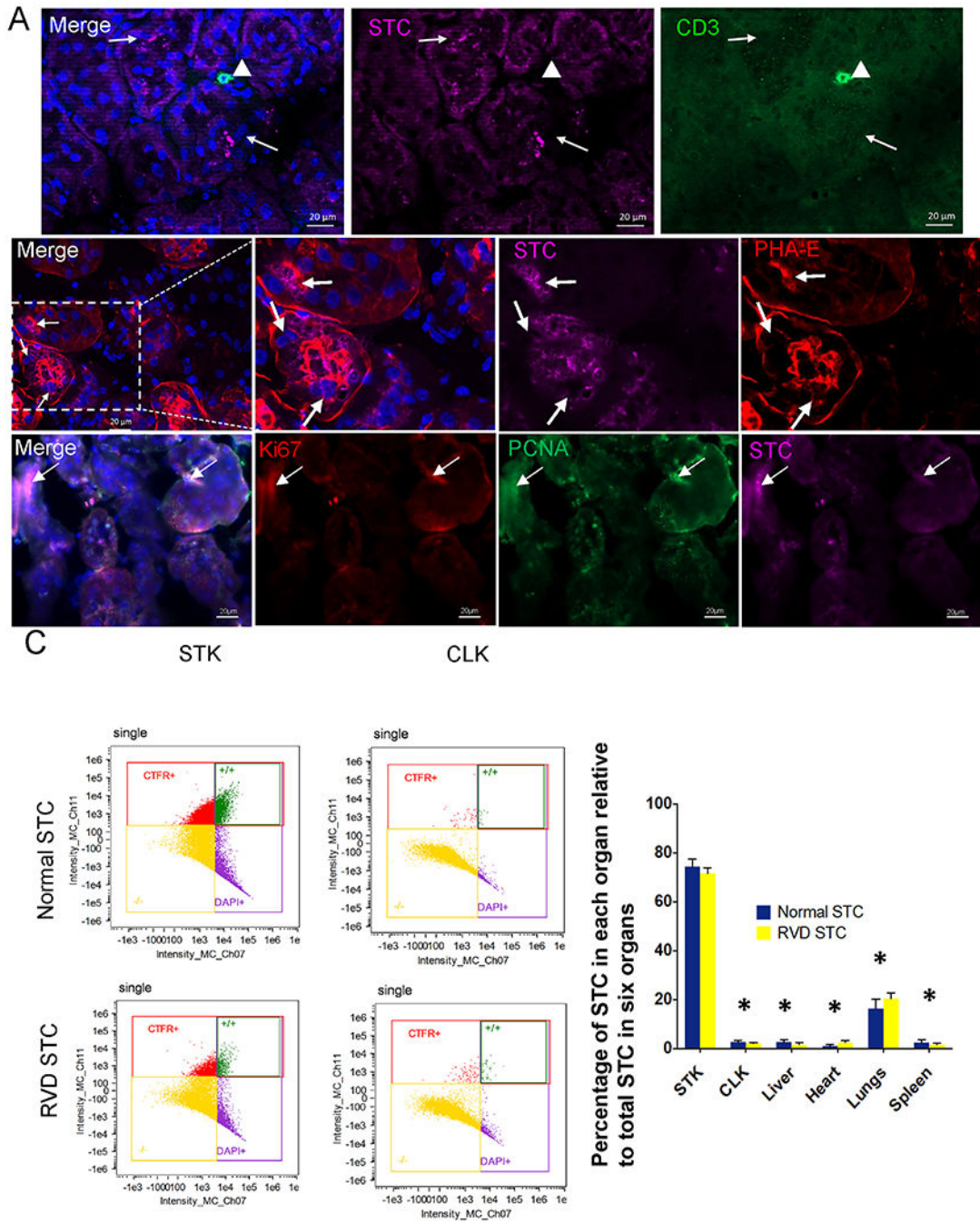


Fig. 3. Transplanted renal scattered tubular-like cells (STC) from Normal and RVD pigs in the murine kidneys. A, Top: Immunofluorescent pre-labeled swine STC (far-red, arrow) do not co-localize with CD3+ T-cells (green, arrowhead) in the murine kidney. Middle: A representative RVD-STC (far-red, arrow) incorporated into renal tubule marked with phaseolus vulgaris erythroagglutinin (PHA-E, red). DAPI: Blue. Bottom: Ki67(red) and PCNA(green) immunostaining showed cell proliferation in engrafted STC. B, Flow cytometry analysis showing the distribution of transplanted cells 2 weeks after injection.

Author Manuscript

Author Manuscript

Author Manuscript

Author Manuscript

Biodistribution of STC detected in the heart, lungs, liver, spleen, stenotic kidney (STK), and contralateral kidney (CLK) was calculated as percentages of the total number of STC detected in those organs. * $p < 0.001$ vs. STK.

Author Manuscript

Author Manuscript

Author Manuscript

Author Manuscript

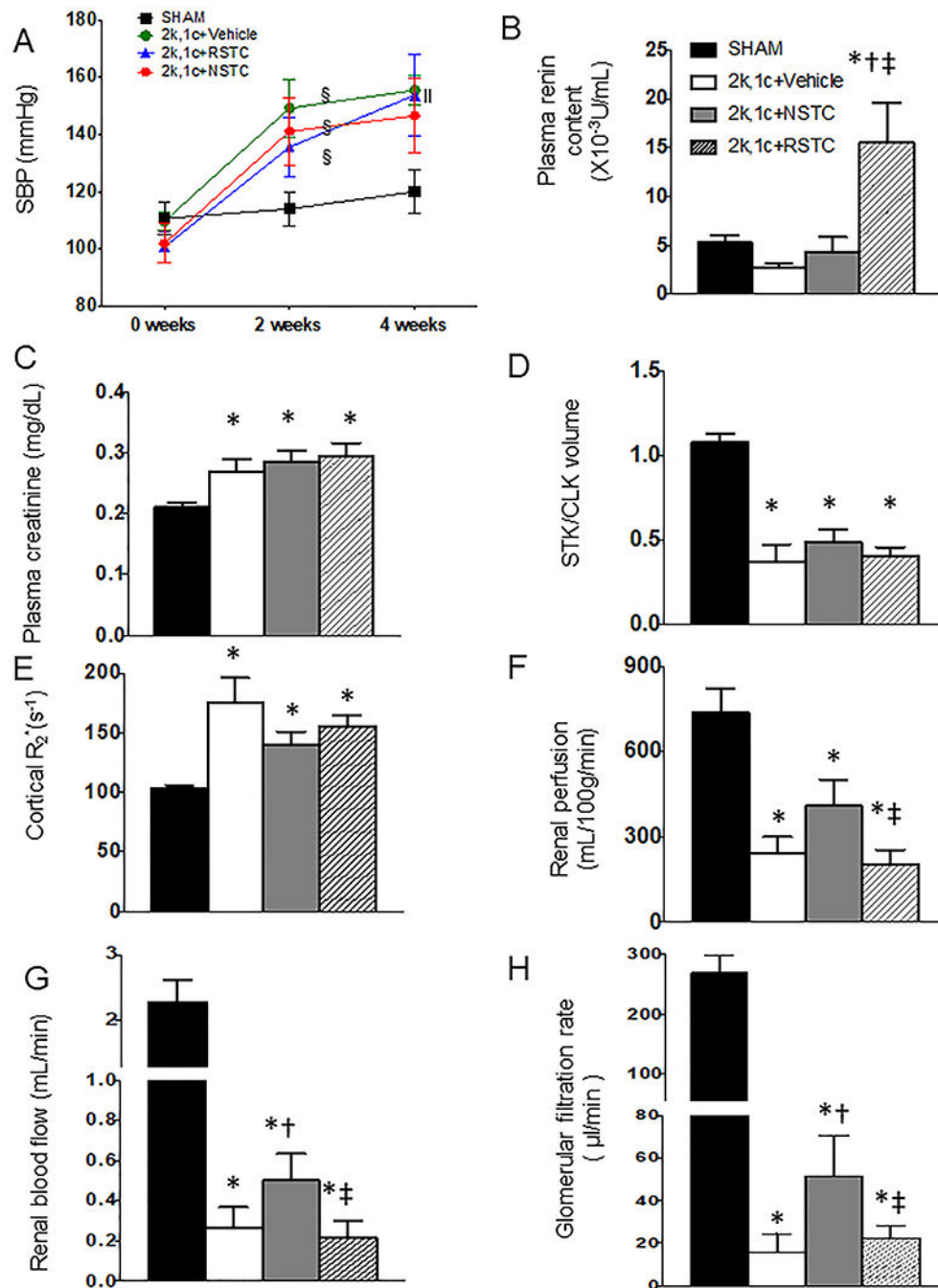


Fig. 4. Systolic blood pressure and renal function (Mean±SD) in sham mice, 2k,1c+Vehicle (V, n=6), 2k,1c+normal STC (NSTC, n=8), and 2k,1c+ RVD-STC (RSTC, n=8) groups. A, Systolic blood pressure. B, Plasma renin content. C, Hypoxia (R_2^* , s^{-1}) by blood oxygen-level-dependent (BOLD) MRI (brighter red represents greater hypoxia). D-F Renal perfusion, blood flow, and GFR by MRI. §p<0.05 vs baseline, §p<0.05 vs 2-week, *p<0.05 vs Sham, †p<0.05 vs 2k,1c+Vehicle, ‡p<0.05 vs 2k,1c+NSTC.

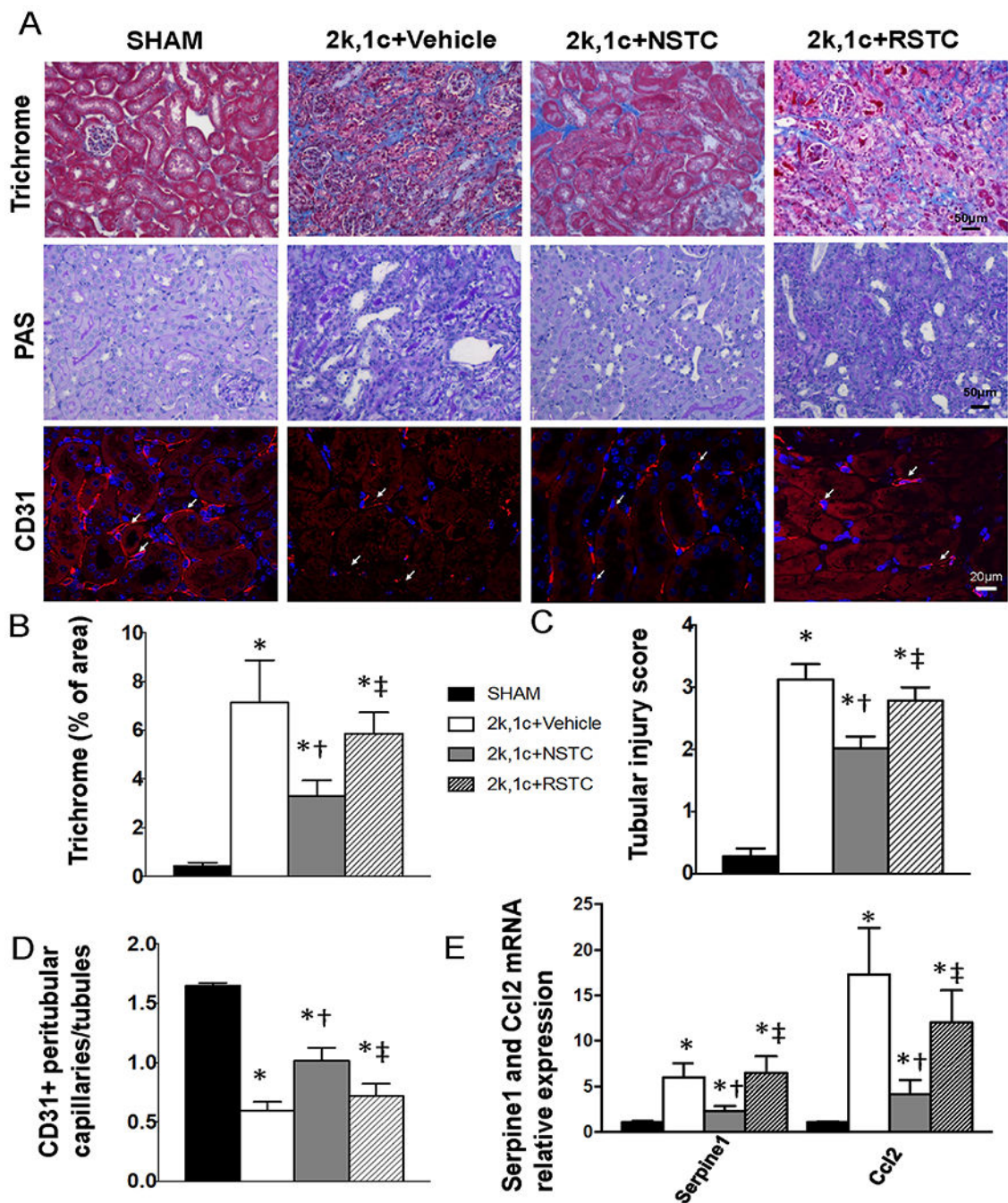


Fig. 5. Renal tissue injury in sham (n=6), 2k,1c+Vehicle (n=6), 2k,1c+normal STC (NSTC, n=8), and 2k,1c+ RVD-STC (RSTC, n=8) mice. A,B, Trichrome staining and quantification of fibrosis. A,C, PAS staining and quantification of renal tubular injury. A,D, Immunofluorescence staining and quantification of CD31+ endothelial cells, denoting microvessels. E, Gene expression of SASP factors *serpine1* and *ccl2* quantified by RT-PCR

(relative to Tbp). Mean±SD; *p<0.05 vs Sham, †p<0.05 vs 2k,1c+Vehicle, ‡p<0.05 vs 2k,1c+NSTC.

Author Manuscript

Author Manuscript

Author Manuscript

Author Manuscript